# Supporting Information for

## Nitrogen Dopants Induced Highly Selective CO$_2$ Reduction over Lotus-leaf Shaped ZnO Nanorods

Fang Lü[a†], Haihong Bao[a†], Fei He[b†], Gaocan Qi[a]*, Jiaqiang Sun[c], Shusheng Zhang[d], Longchao Zhuo[e], Hui Yang[a]*, Guangzhi Hu[f], Jun Luo[a], and Xijun Liu[g]*

[a] Tianjin Key Lab for Photoelectric Materials & Devices, School of Materials Science and Engineering, Tianjin University of Technology, Tianjin 300384, China.

[b] Key Laboratory of Chemistry of Plant Resources in Arid Regions, State Key Laboratory Basis of Xinjiang Indigenous Medicinal Plants Resource Utilization, Xinjiang Technical Institute of Physics and Chemistry, Chinese Academy of Sciences, Urumqi, 830011, China.

[c] State Key Laboratory of Coal Conversion, Institute of Coal Chemistry, Chinese Academy of Sciences, Taiyuan 030001, Shanxi, China.

[d] College of Chemistry, Zhengzhou University, Zhengzhou 450000, China.

[e] School of Materials Science and Engineering, Xi'an University of Technology, Xi'an 710048, Shanxi, China.

[f] College of Biological, Chemical Sciences and Engineering, Jiaxing University, Jiaxing, Zhejiang 314001, China.

[g] Key Laboratory of Civil Aviation Thermal Hazards Prevention and Emergency

Response, Civil Aviation University of China, Tianjin 300300, China.

*Corresponding author

E-mail: xjliu@tjut.edu.cn; gaocanqi@tjut.edu.cn; y.hui1021@tjut.edu.cn

**Experimental sections**

**Preparation of materials**

The ZnO nanorods in lotus-leaf shape were synthesized via a facile solution approach. First, ZnO nanoparticle seeds were deposited on ITO conductive glass by dipping in a ZnO colloidal solution. Then, the ITO glass with seeds was placed in a mixed solution containing 0.025 mol L$^{-1}$ Zn(NO$_3$)$_2$ and 0.025 mol L$^{-1}$ hexamethylenetetramine, and heated at 90 $^o$C for 2–3 h to grow the oriented ZnO nanorods. For the lotus leaf-shaped nanostructures, the ITO glass with the oriented ZnO nanorods was immersed in 0.025 mol L$^{-1}$ hexamethylenetetramine solution and heated in a 90 $^o$C water bath for 24 h. A millimeter-sized pinhole was made in the sealed flask to allow the solution to evaporate slowly. The resulting products were finally washed with distilled water several times and then dried at 60 $^o$C for 2 h. Then N-doped ZnO nanorods were obtained by the following N$_2$ plasma treatment process under room temperature for 30 min.

**Materials Characterization**

The morphology and structure of as-synthesized lotus leaf-shaped ZnO and N-doped ZnO nanorods were investigated by field-emission scanning electron microscopy (SEM, Quanta FEG 250), transmission electron microscopy (TEM, JEOL JEM-2100) instruments equipped with energy dispersive X-ray spectroscopy (EDS). Powder X-ray diffraction (XRD) was performed on an X-ray diffractometer (Rigaku SmartLab 9kW) with Cu K$_\alpha$ radiation ($\lambda$ = 0.154598 nm). X-ray photoelectron spectroscopy

(XPS, Thermo Fisher Scientific) was carried with Al $K_\alpha$ radiation source. The calibration was performed by referencing the C 1s peak at binding energy of 284.8 eV. The $CO_2$-sorption isotherms for the ZnO nanorods were obtained by the Brunauer-Emmett-Teller (BET) measurement with an Autosorb-iQ-MP Micromeritics analyzer.

**Electrochemical Reduction of $CO_2$**

All electrochemical measurements were conducted on an electrochemical workstation (CHI 660D) in a typical H-type cell separated by an anion exchange membrane (Nafion-115). A platinum foil and Ag/AgCl electrode were used as counter and reference electrodes, respectively. 0.5 M $CO_2$-saturated $KHCO_3$ aqueous was used as electrolyte for both chambers. The $CO_2$ gas flow was controlled at 2 mL $min^{-1}$. Linear sweep voltammetry (LSV) curves were performed at a scan rate of 10 mV $s^{-1}$ to examine the electrochemical activity in the range between -1.5 and -0.5 V vs. Ag/AgCl. Electrochemical impedance spectra (EIS) were measured in frequency range from 1 M Hz to 0.01 Hz with an amplitude of 5 mV. The measured potential values vs Ag/AgCl were normalized to those vs RHE according to the Nernst equation:

Potential (V vs. RHE) = Applied potential (V vs. Ag/AgCl) + 0.197 V + 0.0591 × pH.


**Product analysis**

Gaseous products were quantitatively analyzed by online gas chromatography (Agilent GC-7890A) equipped with a Poraplot Q column and a molecular sieve column. Gasses were analyzed using flame ionization detector (FID) and thermal conductivity detector (TCD) detectors with $N_2$ carrier gas. The liquid products were

characterized by nuclear magnetic resonance (NMR) (Bruker AVANCE AV III 400) spectroscopy and dimethyl sulfoxide (DMSO, 99.99%) was used as an internal standard for quantification. The Faradaic efficiency (FE) of specific product can be calculated by the following equation:

$FE = (2nC \times V_{CO_2} \times 10^{-3} \times t \times F)/22.4Q$

where n is the exchanged electron numbers to produce species, C is the volume concentration of the gas products, measured by gas chromatography; $V_{CO_2}$ is the $CO_2$ flow rate (= 2 mL min$^{-1}$); t is electrolysis time; F is the Faradaic constant (96485 C mol$^{-1}$); Q is the cumulative total charge for the $CO_2$ reduction reaction.

**Computational details**

Density functional theory (DFT) calculations were performed using the DMol$^3$ package of MS software. The Perdew-Burke-Ernzerhof (PBE) exchange-correlation functional within a generalized gradient approximation (GGA) was employed as an exchange-correlation functional. The ultra-soft pseudopotentials were used to represent the ionic core. The lattice parameters were found to be a = 3.31 Å, c = 5.33 Å. For ZnO modeling, the non-polar (1010) surface structure was modeled by a six-layer slab with a (2 × 2) unit cell, and the polar (0001) surface was modeled by a (3 × 3) unit cell of six layers. 15 Å vacuum spacing was used to model the surface structure. The energy convergence criterion was set to 2 × 10$^{-5}$ eV. The k-point sampling of the Brillioun zone was done using a 5 × 5 × 1 grid for configurations optimization. The Gibbs free energy change ($\Delta G$) of every elemental step was

calculated according to the computational hydrogen electrode model. ΔG is calculated by the equation: $\Delta G = \Delta E + \Delta E_{ZPE} + \Delta G_U - T\Delta S$, where $\Delta E$ is the electronic energy difference directly obtained from DFT calculations, $\Delta E_{ZPE}$ is the zero point energy, T is the temperature (T = 298.15 K), $\Delta S$ is the change in entropy, and $\Delta G_U$ is the free energy contributions related to the applied electrode potential U.
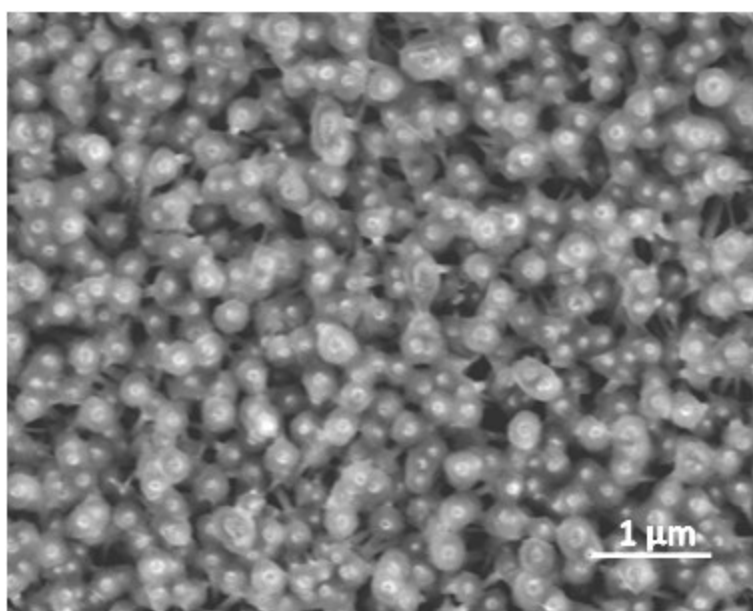
**Fig. S1.** SEM image of lotus leaf-shaped ZnO nanorods.
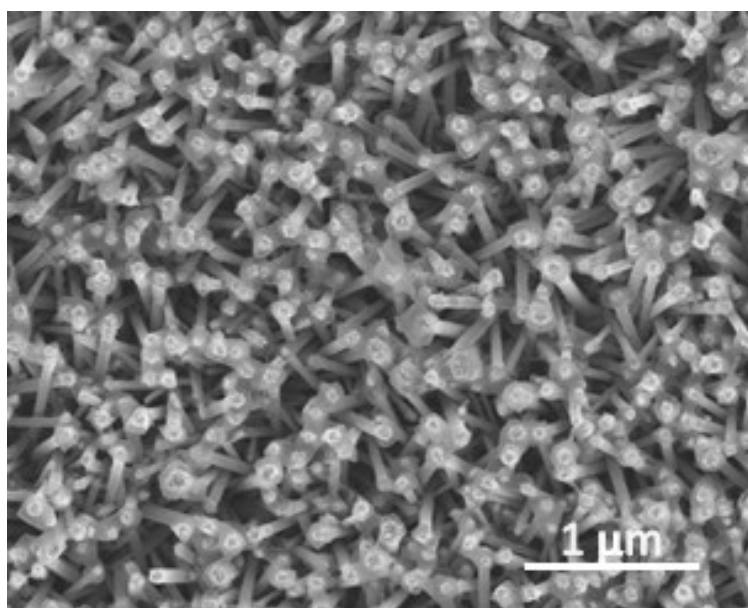
**Fig. S2.** SEM image of N-doped ZnO nanorods in lotus leaf shape.
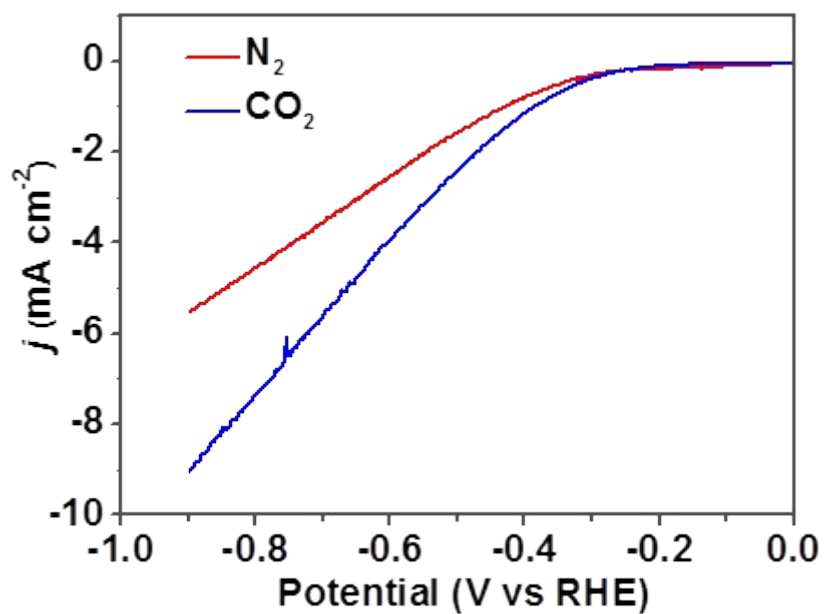
**Fig. S3.** The LSV curves of the electrode based on N-doped ZnO nanorods under $CO_2$ and $N_2$ atmosphere. The blue curve is the same one (blue curve) in Figure 3a.
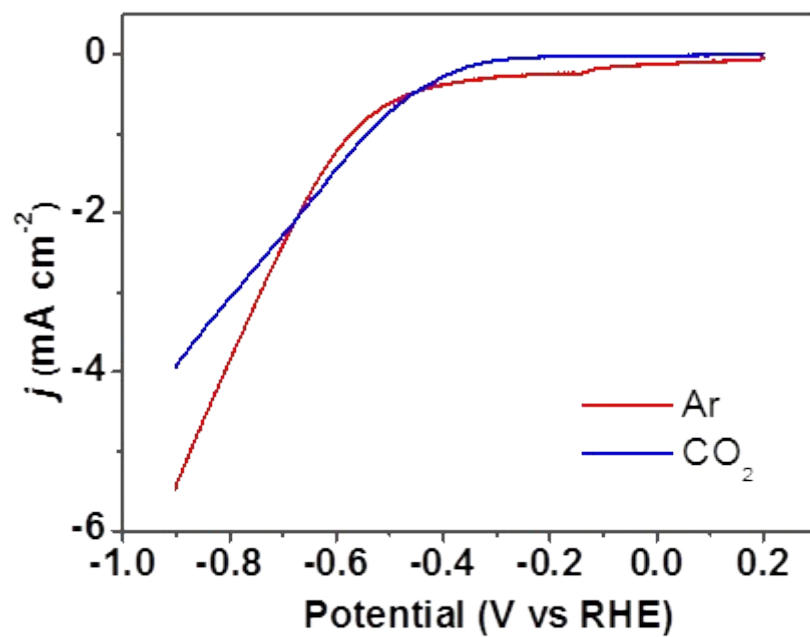
**Fig. S4.** The LSV curves of the electrode based on undoped ZnO nanorods under $CO_2$ and Ar atmosphere. The red curve is the same one (black curve) in Figure 3a.
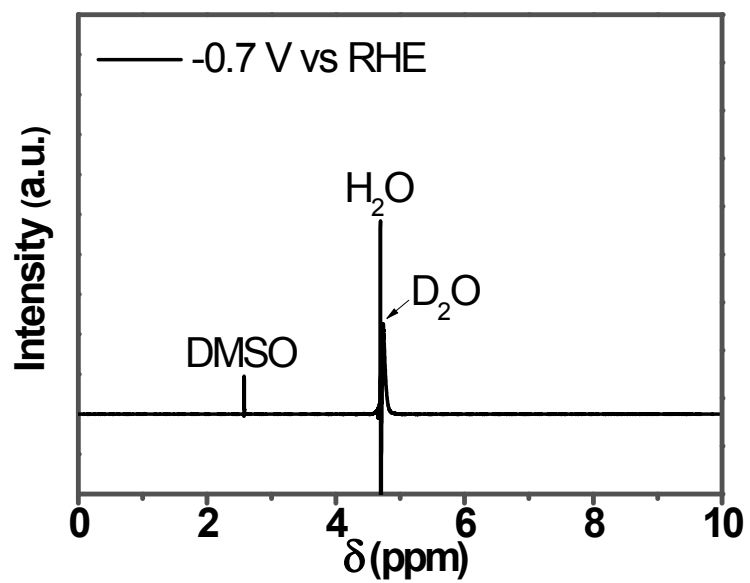
**Fig. S5.** The NMR spectrum of the N-doped ZnO electrode for CO₂RR recorded at - 0.7 V vs RHE. It can be seen that no liquid products were detected.
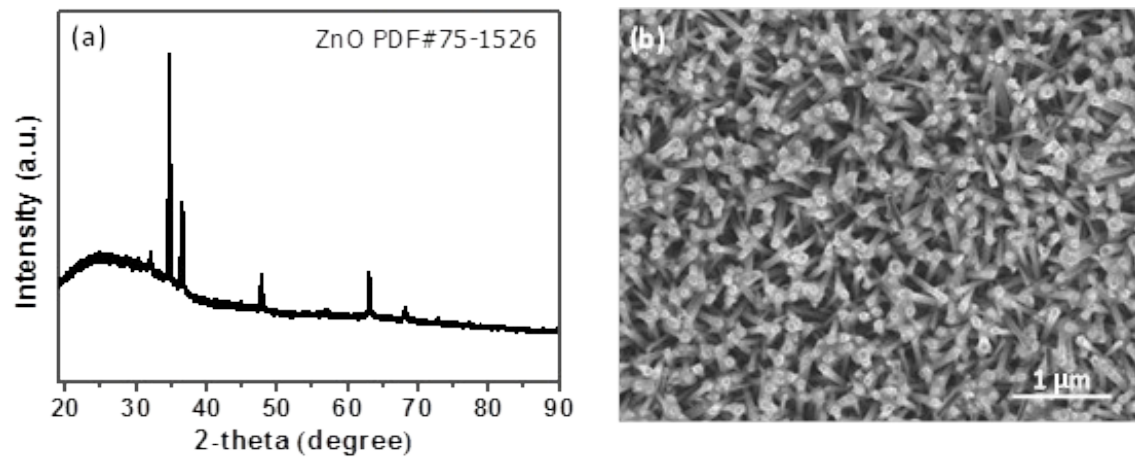
**Fig. S6.** The structure and morphology of N-doped ZnO nanorods after long-term electrocatalysis. (a) XRD pattern, (b) SEM image.
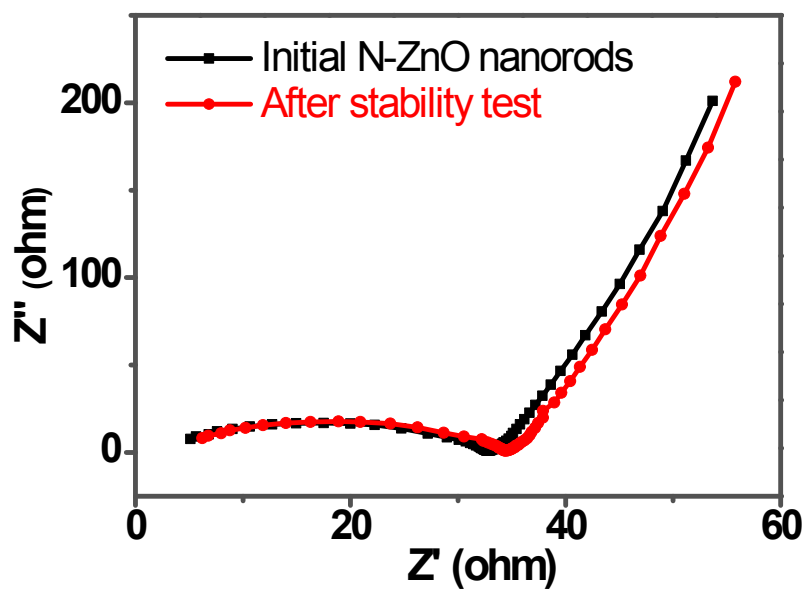
**Fig. S7.** The electrochemical impedance spectroscopy of N-doped ZnO nanorods before and after the long-term electrocatalysis. Clearly, the two curves are close to each other, suggesting the good electrochemical stability of N-doped ZnO nanorods.
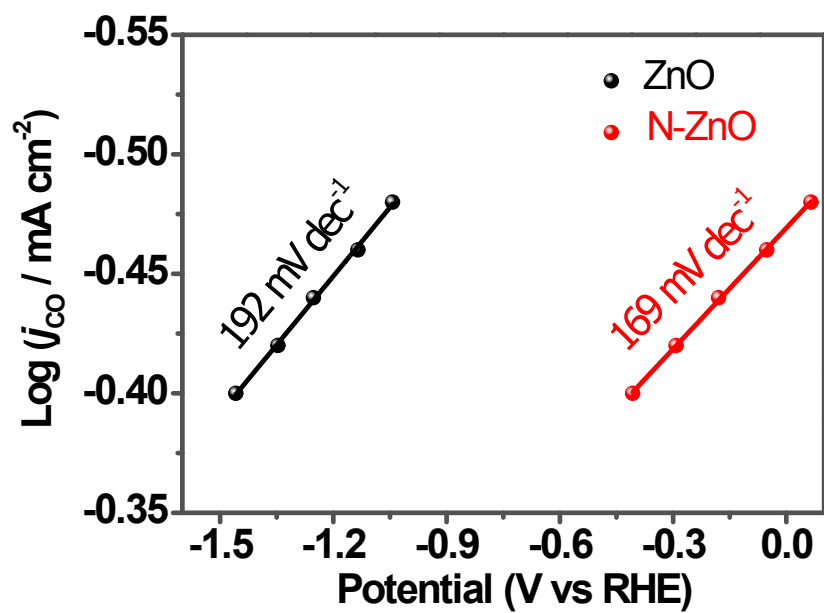
**Fig. S8.** The Tafel plots of the electrodes based on ZnO and N-doped ZnO nanorods.